

On standing sausage waves in photospheric magnetic waveguides

I. Dorotovič,¹ R. Erdélyi,² N. Freij,² V. Karlovský,³ and I. Márquez,⁴

¹ Slovak Central Observatory, P. O. Box 42, SK-94701 Hurbanovo, Slovak Republic
e-mail: ivan.dorotovic@suh.sk

² Solar Physics & Space Plasma Research Centre (SP²RC), School of Mathematics and Statistics, University of Sheffield, Hicks Building, Hounsfield Road, Sheffield, S3 7RH, United Kingdom
e-mail: robertus@sheffield.ac.uk

³ Hlohovec Observatory and Planetarium, Sládkovičova 41, SK-92001 Hlohovec, Slovak Republic e-mail: astrokar@hl.cora.sk

⁴ Instituto de Astrofísica de Canarias, E38205, La Laguna, Tenerife, Spain e-mail: imarquez@ull.es

Received ; accepted

ABSTRACT

Aims. By focusing on the oscillations of the cross-sectional area and the intensity of magnetic waveguides located in the lower solar atmosphere, we aim to detect and identify magnetohydrodynamic (MHD) sausage waves.

Methods. Capturing several series of high-resolution images of pores and sunspots and employing wavelet analysis in conjunction with empirical mode decomposition (EMD) makes the MHD wave analysis possible. For this paper, two sunspots and one pore (with a light bridge) were chosen as representative examples of MHD waveguides in the lower solar atmosphere.

Results. The sunspots and pore display a range of periods from 4 to 65 minutes. The sunspots support longer periods than the pore – generally enabling a doubling or quadrupling of the maximum pore oscillatory period. All of these structures display area oscillations indicative of MHD sausage modes and in-phase behaviour between the area and intensity, presenting mounting evidence for the presence of the slow sausage mode within these waveguides.

Conclusions. The presence of fast and slow MHD sausage waves has been detected in three different magnetic waveguides in the lower solar photosphere. Furthermore, these oscillations are potentially standing harmonics supported in the waveguides which are sandwiched vertically between the temperature minimum in the lower solar atmosphere and the transition region. Standing harmonic oscillations, by means of solar magneto-seismology, may allow insight into the sub-resolution structure of photospheric MHD waveguides.

Key words. Sun: atmosphere – Sun: oscillations – Sun: sunspots – Sun: photosphere

1. Introduction

Over the past decades, many oscillatory phenomena have been observed within a wide range of magnetic waveguides in the solar atmosphere (Banerjee et al. 2007; Wang 2011; Asai et al. 2012; Arregui et al. 2012). Sunspots and pores are just two of these many structures and they are known to display solar *global* oscillations, see a recent review by e.g. Pintér & Erdélyi (2011).

The commonly studied oscillatory periods in sunspots: 3 and 5 minutes. These oscillations are seen in intensity, line of sight (LOS) velocity and LOS magnetic field. The source of the 5-minute oscillation is a result of forcing by the 5-minute (*p*-mode) global solar oscillation, which forms the basis of helioseismology (Thompson 2006). The 5-minute oscillations are typically seen in simple molecular and non-ionized metal lines, which form low in the umbral photosphere and are moderately suppressed not only in the penumbra, but also in the chromospheric atmosphere above the umbra (Bogdan & Judge 2006). The cause of the 3-minute oscillations is still unknown but there are two main streams of theories: they could either be standing acoustic waves which are linked to the resonant modes of the sunspot (Bogdan & Judge 2006) or they could be low- β slow magneto-acoustic-gravity waves guided along the ambient magnetic field (Bogdan 2000). The 3-minute oscillations are seen in plasma elements that form higher up, in the low chromosphere, and these are also moderately suppressed in the

penumbra (Christopoulou et al. 2000; Bogdan & Judge 2006; Kobanov et al. 2006).

Magnetohydrodynamic (MHD) theory, when applied to a cylindrical magnetic flux tube, reveals that a variety of waves can be supported, four of which are often reported in various structures in the solar atmosphere. Longitudinal (slow sausage) (de Moortel 2009; Wang 2011), fast kink (Andries et al. 2009), fast sausage (McAteer et al. 2003) and Alfvén (torsional) waves (Jess et al. 2009), each of which affects the flux tube in a specific way. The sausage modes are of interest here; the sausage mode is a compressible, symmetric perturbation around the axis of a flux tube which causes density perturbation that can be identified in intensity images (Edwin & Roberts 1983). Furthermore, due to the fact that the wave will either compress or expand the flux tube, the magnetic field will also show signs of oscillations. This mode may come in two forms in terms of phase speed classification: a slow mode (often also called the longitudinal mode) which generally has a phase speed close to the characteristic tube speed and a fast mode, which has a phase speed close to the external sound speed, assuming a region that has a plasma- $\beta > 1$ (Erdélyi 2008). The main difference between the two modes is the phase relationship between appropriate MHD quantities which allows them to be identified. In this case, the fast sausage mode has an out-of-phase relationship between the area and intensity, while the slow sausage mode has an in-phase relationship. The technique that was applied to obtain these phase re-

relationships are covered by e.g. Goedbloed & Poedts (2004) and Fujimura & Tsuneta (2009).

Sausage modes have been observed in solar pores; Dorotovič et al. (2008) observed a pore for 11 hours and reported periodicities in the range of 20-70 minutes. These oscillations were consequently interpreted as linear low-frequency slow sausage waves. Morton et al. (2011) used the Rapid Oscillations in the Solar Atmosphere (ROSA) instrument to also identify linear sausage oscillations in a magnetic pore. However, determining whether the oscillations were slow or fast proved to be difficult.

The source and driving mechanism(s) of these MHD sausage modes have been very difficult to identify. Numerical simulations of a flux tube rooted in the photosphere are buffeted by a wide range of coherent sub-photospheric drivers. These drivers can either be horizontal or vertical, single, paired or a power spectrum, with varying phase differences (see e.g. Malins & Erdélyi 2007; Khomenko et al. 2008; Fedun et al. 2011a,b). One example of a horizontal driver representing solar global oscillations is the absorption of the global p -mode by the magnetic field of the sunspot. Mathew (2008) studied this effect and found a structured ring-like absorption pattern in Doppler power close to the umbral-penumbral boundary. This effect was largest where the transverse magnetic field was at its greatest and this region allows fast waves to be converted into slow magneto-acoustic waves, which are a potential source of MHD waves in sunspots and other similar magnetic structures.

We report here, the observation of both *slow* and potentially, *fast* sausage MHD waves in the lower solar atmosphere on three different occasions and in magnetic waveguides of various types. In section 2, we describe the data collection and the data processing method. In section 3, we describe the results obtained from the three different data series and discuss the findings. Section 4 details the underlying idea of identifying these oscillations as *standing* harmonics. Finally, in section 5, we conclude.

2. Data collection and Method of Analysis

Three time series of images with high angular resolution have been chosen here, in order to demonstrate the identification of MHD sausage waves. The images were taken in the G band (4305 Å), which samples the low photosphere, and were acquired using:

1. The Swedish Vacuum Solar Telescope (SVST) situated in La Palma on the Canary Islands. Scharmer et al. (1985) provides a detailed description of the features of the SVST. The images were taken on the 7th July 1999. The sunspot is in the Active Region NOAA 8620. The observing duration is 133 minutes with a cadence time of 25 seconds. The field of view covered an area of 33,600 km by 54,600 km (1 pixel \approx 60 km). Bonet et al. (2005) gives a detailed analysis of this sunspot. A context image is the left image of Fig. 1.
2. The Dutch Open Telescope (DOT), is also situated in La Palma on the Canary Islands. Two series of imaging data sequences were taken using this telescope. A detailed guide of the features of the DOT is provided by Rutten et al. (2004). The first series of data was taken on the 13th July 2005; the sunspot is in the Active Region NOAA 10789. The region has been slowly decaying and this sunspot is leading the small group. The observing period is 165 minutes and has a cadence time of 30 seconds. The second set of data, taken on the 15th October 2008, is of one large pore with a light bridge which is about 15 pixels (750 km) wide in the

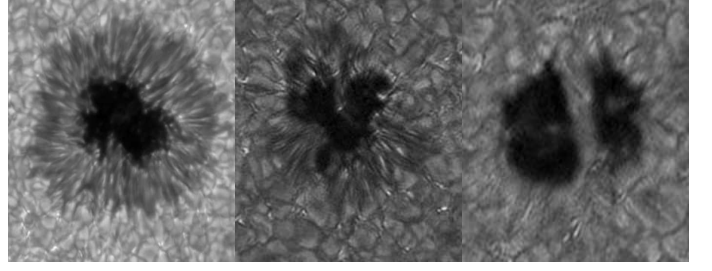


Fig. 1: An overview of the magnetic waveguides observed for this analysis. (*left*) The 1999 sunspot observed with the SVST with an average umbral area of 19,650 pixels (50 Mkm^2). (*middle*) The 2005 sunspot observed with the DOT with an average umbral area of 12,943 pixels (32 Mkm^2). (*right*) The 2008 pore observed with the DOT with an average area of 10971 pixels (27 Mkm^2), the light bridge that separates the pore can be seen. Furthermore, these structures were seen near the disk centre, so there is little to no line of sight effects.

Active Region NOAA 11005. The duration of the observing run is 66 minutes and has a cadence time of 20 seconds. Both DOT image sequences covered an area of 50,000 km by 45,000 km, where the maximum spatial resolution is $0.2''$ ($\approx 140 \text{ km}$). Typical context images are the middle and right panels of Fig. 1.

In order to obtain information relating to the cross-sectional area of these waveguides, a strict and consistent definition of the area is required - each pixel has a value of less than 3σ of the median background intensity. The background is defined as an area of the image where there is no formed magnetic structure. This may appear to be an arbitrary definition, however, a histogram of the background intensity reveals a Gaussian distribution and when adding the area around and including the waveguide, there is significant peak on the lower end of the Gaussian distribution curve around 3σ or higher. Thus, we have a 99% confidence that the area is of the structure and not of the background. The mean intensity value was determined by summing over the intensity of each pixel found in the waveguide and dividing it by the total estimated area. These waveguides are not static structures, they slowly changed in size during the observing period. This slowly varying size change had to be removed in order for it not to mask any weaker oscillation signatures. The detrending was accomplished by a non-linear regression fit and the consistency of the results was compared to subtracting the residue from an Empirical Mode Decomposition (EMD) analysis (explained below). The residue is the data that remains after the EMD procedure has extracted as many signals as possible and it provides a very good approximation of the background trend.

The resulting reduced data series were then analysed with a wavelet tool in order to extract any periods of oscillation present within the data. The algorithm used is an adapted version of the IDL wavelet routine developed by Torrence & Compo (1998). The standard Morlet wavelet, which is a plane sine wave with an amplitude modulated by a Gaussian function, was chosen due to its suitable frequency resolution. Furthermore, both white and red noise backgrounds were employed in order to verify the consistency of the results. The cross-hatched area marks the cone of influence (COI), where edge effects due to the wavelet structure affect the wavelet transform and anything inside the COI is discarded. The contours show the confidence level of 95%. Further to this, the data representing the size and intensity has also been

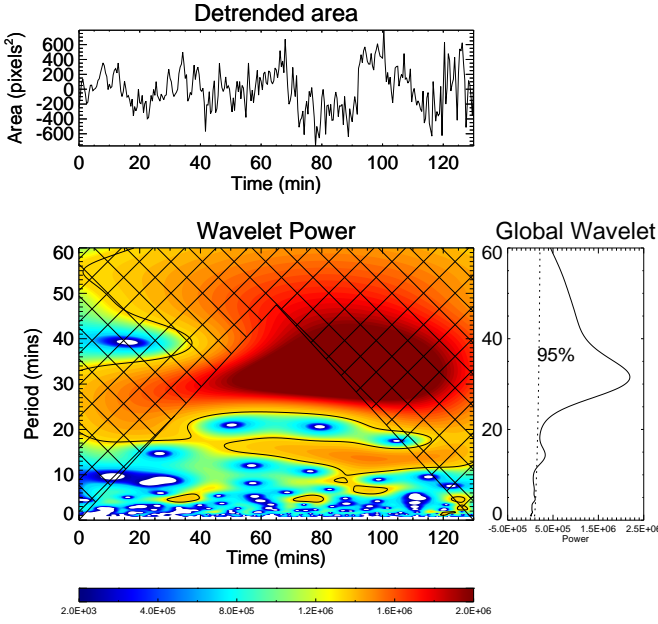


Fig. 2: Evolution of the area of the 1999 sunspot (*upper panel*); the wavelet power spectrum for a white noise background, the cone of influence is marked as a cross-hatched area where edge effects become important and the contour lines show the 95% confidence level (*lower left panel*). Global (integrated in time) wavelet power spectrum, where the dashed line shows the 95% confidence limit (*lower right panel*).

analysed using EMD, which decomposes the time series into a finite number of Intrinsic Mode Functions (IMFs). These are essentially narrowband filtered time series, with each IMF containing one or two periods that exist in the original data series. For more information on the features and applicability of the EMD method see e.g. Terradas et al. (2004). The EMD technique was first proposed by Huang et al. (1998) and offers certain benefits over more traditional methods of analysis, such as wavelets or Fourier transforms. Generally, the next step after EMD analysis is to construct a Hilbert power spectrum which has a better time and spatial resolution than either wavelet or FFT routines. However, this has not been carried out due to a lack of a robust code base at this time and will be addressed in future work. At this stage, we rely on wavelet and EMD analyses, as customary in solar physics.

3. Results and Discussion

3.1. Sunspot, 7 July 1999, AR 8620

Fig. 2 shows the wavelet analysis of the 1999 sunspot area data. There are three confidently identified periods that exist with 95% certainty; 5, 14 and 32 minutes. The 32-minute period is found over a wide range of the time series, with some of its power inside the COI. However, most is confidently outside the COI. The 14-minute period is highly localised at around 50 to 120 minutes of the data series and it appears to be an off shoot of the 32-minute period. The 14-minute period starts at 17 minutes and it slowly decays and stabilizes at 14 minutes. The 5-minute period is relatively weak compared to the other two periods and there are regions of strong power where the period is either greater or

lower than 5 minutes and this could be indicative of the 3-minute oscillation.

The intensity wavelet shows three distant periods of oscillations: 6, 24 and 33 minutes. The 6- and 33-minute periods both correspond to two of the area wavelet oscillations, however, the 24-minute oscillation is not seen in the area wavelet. Some effect must therefore be causing the disparity in oscillation periods, perhaps the opacity effect (see Fujimura & Tsuneta 2009). It is safe to say that these oscillations are caused by sausage waves. The reason is that in standard MHD theory, the sausage wave is the only MHD wave capable of changing the area of the flux tube that is observed on disk (see e.g. Cooper et al. 2003a,b).

Without the ability to directly compare the area to intensity, great caution needs to be exercised to determine with confidence whether the perturbations are fast or slow. A wavelet phase diagram reveals regions (where the wavelet coherence is high and the period is ≤ 20 minutes) to be either out-of-phase or in-phase but a clear image of constant phase difference does not appear. This might be due to mode conversion occurring in the sunspot, since the G-band samples a region where plasma- β is ≈ 1 in a magnetic structure (Gary 2001). When the period is ≥ 20 minutes, the only area of high coherence is located around 32 minutes and found to be out-of-phase, which hints that there is a fast sausage wave. However, only two full wave periods are outside the COI, which is due to the total length of the data series.

Fig. 3 shows the computed IMFs for the 1999 sunspot data set. The IMFs show the periods of oscillations identified using the EMD routine. Six IMFs are shown, two were neglected due to uncertainties and the additional residue is ignored. In general, the higher order IMFs tend to show longer periods and as such contain fewer wave periods, which makes phase identification less reliable. In this case, only two IMFs coincide (c_3 and c_6) with the wavelet period that shows both area and intensity perturbations. IMF c_3 shows a period of 5 minutes and contains several regions of three or more wave periods that are either in- or out-of-phase behaviour which agrees with the cross-wavelet phase analysis. IMF c_6 has clear out-of-phase behaviour between the area and intensity for first three wave periods, which is potentially indicative of a fast MHD sausage wave.

It was possible to approximately separate the penumbra from the umbra and investigate its area for oscillations. However, the penumbra is a highly dynamic object and this makes the area estimation reasonably uncertain. There seem to be four periods that exist at 95 % certainty: 7, 14, 25 and 44 minutes. The longest period happens to have the majority of its power inside the COI, so it has been discounted. The 26-minute period is mostly concentrated at the start of the time series but as time evolves forward, the power starts to decay and the period drops to 20 minutes. This change in period is most likely caused by the decay of the sunspot over the observational period and the fact that the magnetic flux slowly decays along with it. The two shorter periods (7 and 14 minutes) closely correspond to the 5- and 14-minute oscillations in the umbra; they could be a continuation of these umbral periods that became up-shifted as they enter the less compact structure of the penumbra. The EMD analysis of the penumbral oscillations reveals that area oscillates in-phase with the intensity. No signal of fast sausage MHD wave is seen; this indicates in this case that mode conversion has not occurred in this region.

3.2. Sunspot, 13 July 2005, AR 10789

Fig. 4 shows the wavelet analysis of the 2005 sunspot area in AR 10789. There are six periods that exist at 95 % confidence

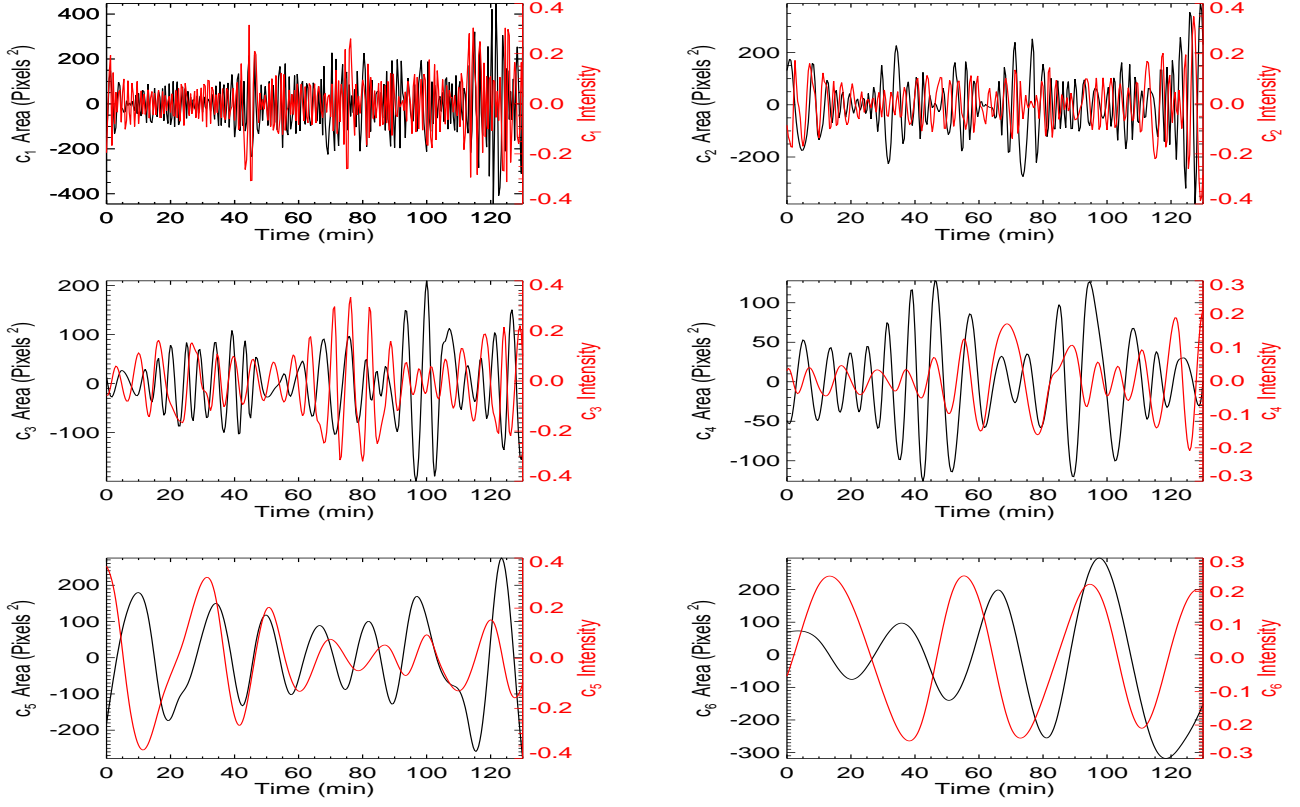


Fig. 3: The IMFs of the evolution of the area (red) and intensity (black) for the 1999 sunspot, over-plotted to aid comparison. Generally after the 6th IMF, higher IMFs lack a sufficient number of wave periods, which makes it difficult, and less reliable, to obtain an accurate period.

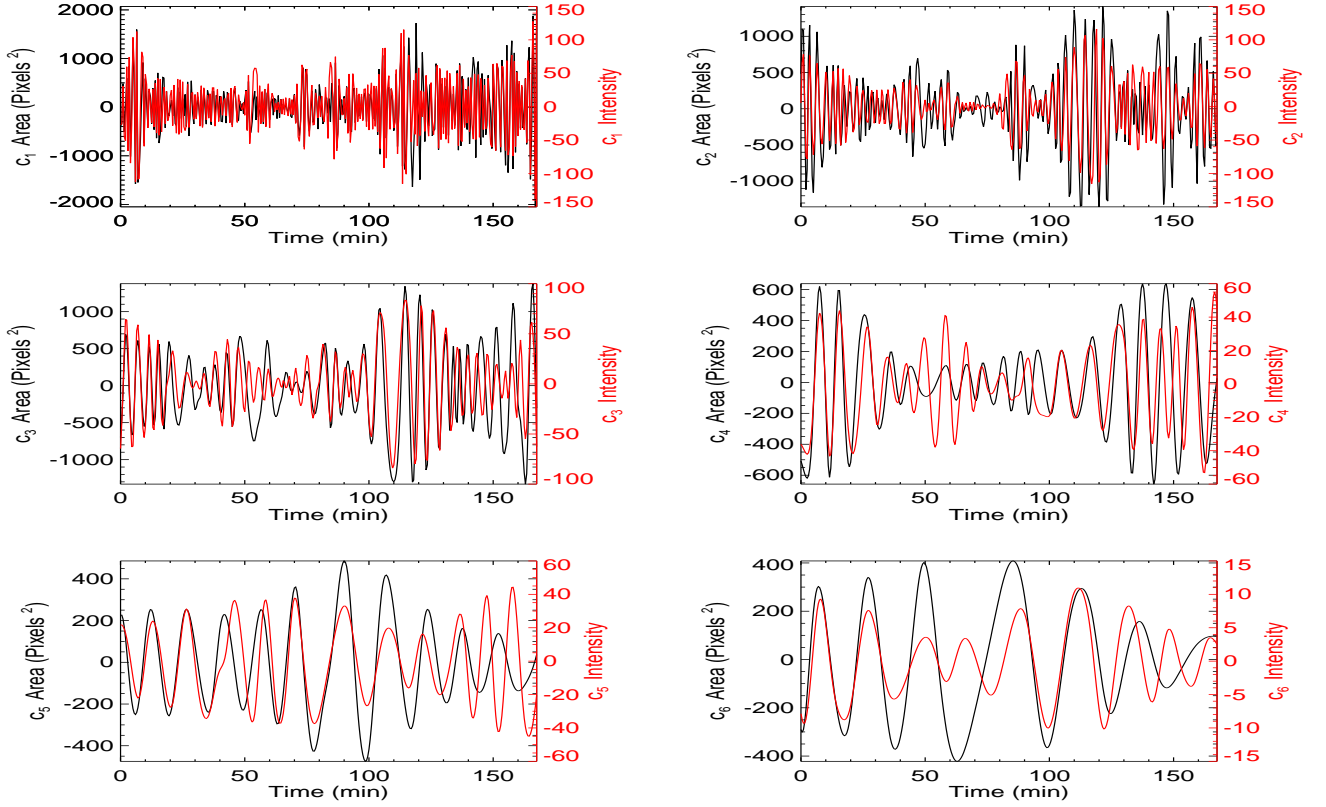


Fig. 5: Same as Fig. 3 but for the sunspot in Active Region 10789 in 2005.

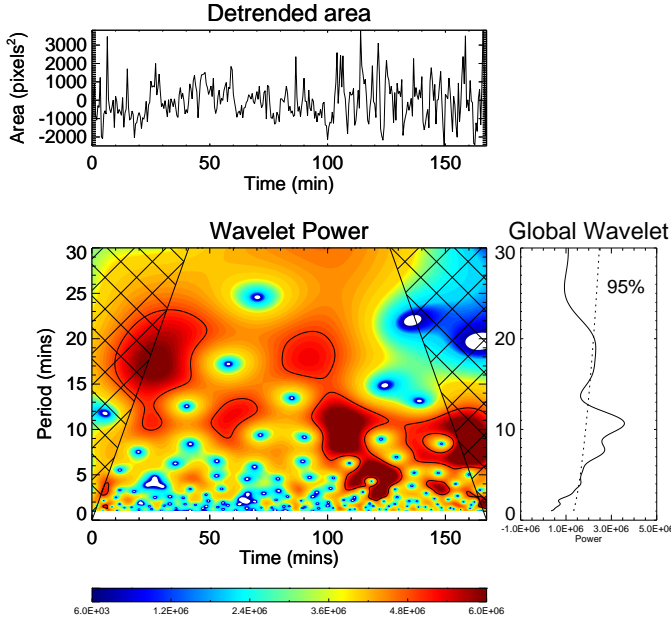


Fig. 4: Same as Fig. 2 but for the sunspot in Active Region 10789 in 2005.

level: 4, 5.5, 7.5, 10.5, 17.5 and 65 minutes. The longest period has its wavelet power reach a maximum value at 65 minutes but the power is spread from 50 to 80 minutes and, in this case, it is inside the COI and so it has been neglected for further analysis. A comparison with the corresponding intensity wavelet reveals that the intensity shows 7.5, 10.5, 21 and 65-minute oscillations. The cross-wavelet phase indicates that these oscillations are in-phase. There appears to only be very small and infrequent regions of out-of-phase behaviour that occur for 1 to 2 wave periods at around periods of 2 to 3 minutes. This is most likely an artefact of the wavelet transform at very low periods.

Fig. 5 shows the IMFs for the area and the intensity of the sunspot data in AR 10789. Only c_3 and c_4 show oscillations that occur in the area and the intensity time series. The region of interest is within the time interval of 90-130 minutes, where the wavelet has these oscillations. Both IMFs show clear in-phase behaviour in this time interval and both have one wave period out-of-phase at around 110 minutes. The overall phase relation between the area and intensity indicates the presence of slow sausage waves.

3.3. Pore, 15 October 2008

Fig. 6 shows the wavelet analysis of the pore with a light bridge. There are three periods that exist at 95 % confidence level: 4.5, 8.5 and 14.5 minutes. The majority of the power of the period of 14-15 minutes is inside the COI and so this period has been discarded. The other two periods: 4.5 and 8.5 minutes are seen in both area and intensity data when the wavelet analyses are cross-correlated. The power for these two periods is concentrated in the time interval of 20-60 minutes. The cross-wavelet analysis shows that the overlapping time span is somewhat smaller, at about 30-50 minutes.

Fig. 7 shows the IMFs for the area with intensity overplotted. In this case, c_3 indicates a period of 4.5 minutes and c_5 has a characteristic period of 8.5 minutes; this applies to both

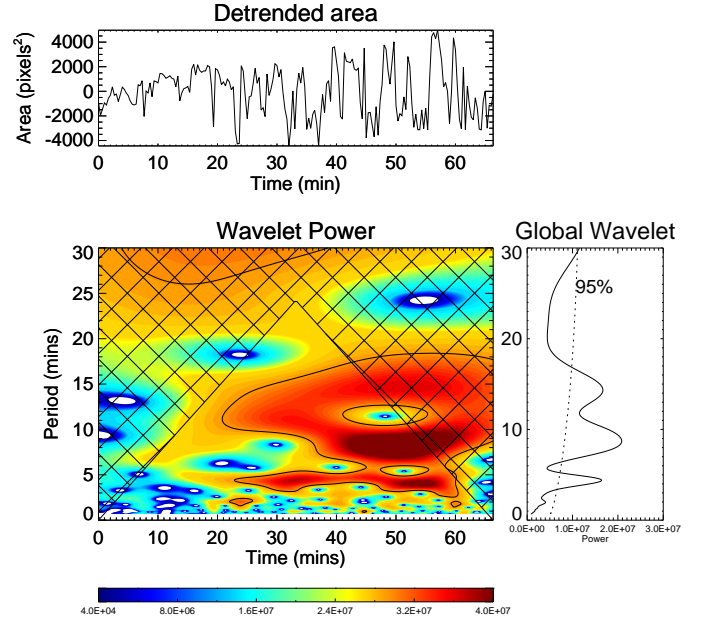


Fig. 6: Same as Fig. 2 but for the pore in Active Region 11005 in 2008.

the area and intensity IMFs. c_3 reveals that the phase relation is out-of-phase for about three wave periods, with a period of in-phase behaviour only at either end of this group for the time interval 20-40 minutes. This behaviour occurs twice more in this IMF. The comparison of c_5 also reveals that the phase relation is out-of-phase for about 2 wave periods and shows a small region of in-phase behaviour at the end of this time series. Once again, this behaviour is a potential indicator of the presence of fast sausage MHD waves in this pore.

Let us make a few general comments apply to all the results. The easiest way to confirm the linearity of waves is to compare the amplitude of the oscillations to the characteristic scale of the structure. In all three cases studied here, the oscillation amplitudes are around 10% or less of the total area, which indicates that these oscillations are linear. Furthermore, the amplitude of the oscillation in these three cases is roughly the same. So the amplitude scales with the size of the structure.

4. Standing Harmonics

Basic MHD theory interpretation allows sunspots and pores to be described as vertical cylindrical flux tubes, with the base bounded in the photosphere and the top bounded at the transition region due to the sharp gradients in the plasma properties at these locations (Luna-Cardozo et al. 2012). Taking this further, an ideal flux tube is assumed here. The plasma density and magnetic field are homogeneous within the flux tube. This means that the standing harmonics of such flux tubes are the MHD equivalent to those of the harmonics in an open-ended compressible air pipe, where the ratio of the harmonic periods is given by, $P_1/P_2 = 2$, $P_1/P_3 = 3$ and so forth.

Let us now summarise the observed findings. Table 1. contains the periods of oscillations found in all three magnetic waveguides.

For the 1999 sunspot, there are 3 periods found. The second period at 14 minutes gives a period ratio (P_1/P_2) of 2.3 ± 0.3 ,

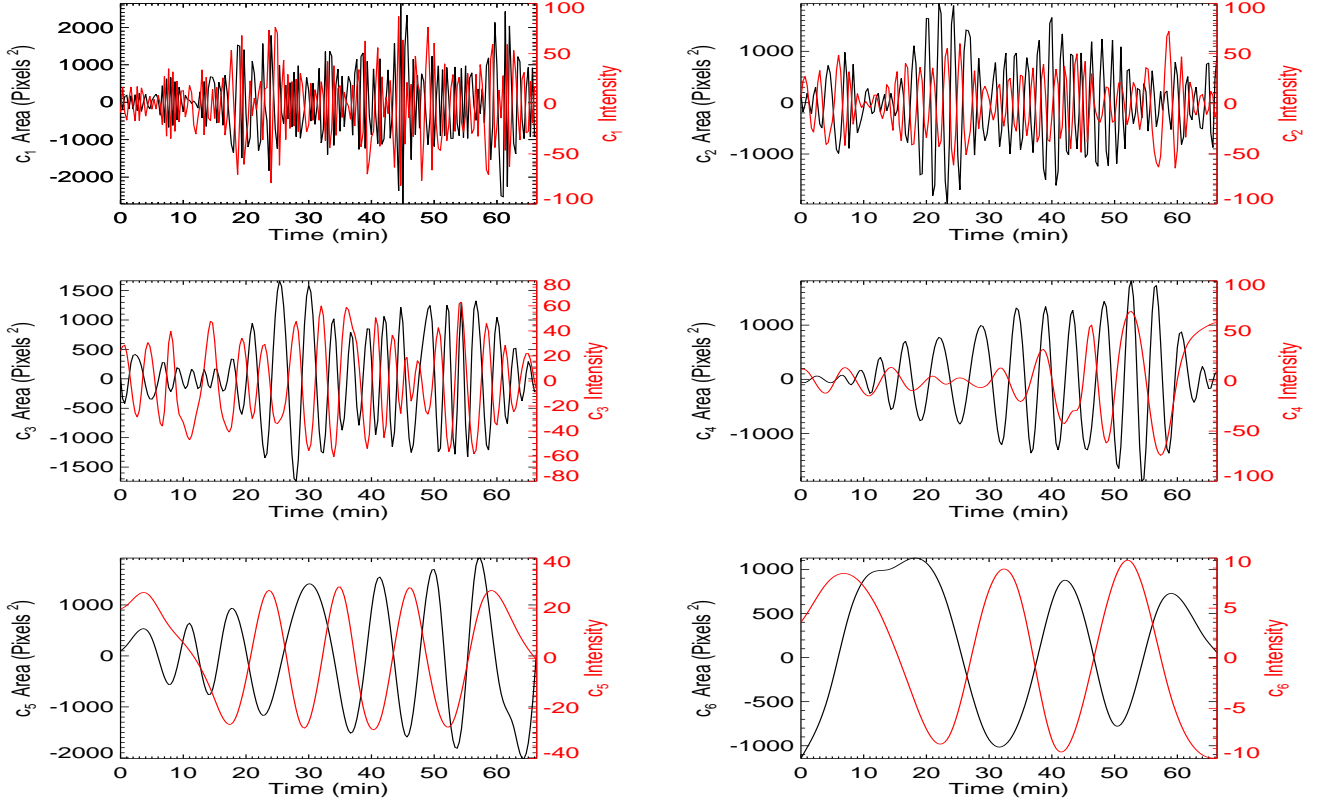


Fig. 7: Same as Fig. 3 but for the pore in Active Region 11005 in 2008.

Data Set	Period (Mins)	Ratio (P_1/P_i)
Sunspot 1999	$P_1 - 32 \pm 3$	-
	$P_2 - 14 \pm 1$	2.3 ± 0.3
	$P_3 - 5 \pm 0.5$	6.4 ± 0.9
Sunspot 2005	$P_1 - 17.5 \pm 1.5$	-
	$P_2 - 10.5 \pm 0.5$	1.7 ± 0.2
	$P_3 - 7.5 \pm 0.5$	2.5 ± 0.3
	$P_4 - 5.5 \pm 0.5$	3.2 ± 0.4
	$P_5 - 4 \pm 0.5$	4.4 ± 0.7
Pore 2008	$P_1 - 8.5 \pm 0.5$	-
	$P_2 - 4.5 \pm 0.5$	1.8 ± 0.2

Table 1: The periods of oscillations that are found in the area of the waveguides that exist at 95% confidence level and are outside the COI. There is another period for the 2008 pore which is discussed in the text but not included in the table due to the criteria laid out.

which is slightly higher than the expected value of a uniform waveguide with a canonical value of 2 but it is within the error range. The other period is more controversial to fit into this image. The 5 minute period has a ratio that is maybe too high to incorporate into a harmonic standpoint and begs the question: where are the other harmonics in-between? It is more plausible that this 5 minute period is just a result from the global p -mode buffeting the magnetic waveguide.

For the 2005 sunspot in AR 10789, there is a clearer picture of potential harmonics. The first period is at 17.5 minutes and the second period is at 10.5 minutes, which gives a ratio of 1.7 ± 0.2 , and the third period at 7.5 minutes gives a ratio of 2.5 ± 0.3 . The period ratio is modified downwards in a consistent

manner, by 0.2 or 0.3 as the harmonic number increases. These ratios are strong evidence for standing waves in this magnetic waveguide. The last two periods (5.5 and 4 minutes) are again too close to the global p -mode oscillation period. However, the 5.5 minute period still fits the pattern for the decreasing period ratio whereas the last period breaks this pattern.

For the 2008 pore of AR 11005, the picture is more muddled due to the short time series available. The 15 minute period has been ignored due to having the majority of its power inside of the COI but is more likely to be the first harmonic than the 8.5 minute period. Assuming that the 8.5 minute period is the first harmonic, the ratio is 1.8 for the 4.5 minute period, which happens to be very similar to the ratio of the 2005 sunspot's first period ratio. If we ignore the issue with the 14.5 minute period for the time being, it alters the period ratios to 1.7 and 3.2 for 8.5 and 4.5 minutes respectively. This result makes more sense as it is more likely that any observation of periods around 5 minutes is a direct result of the global p -mode oscillation and this brings the second period ratio into line with the 2005 sunspot period ratio.

The main conclusion to take away from this data analysis so far is that the simple homogeneous flux tube model cannot fully account for these ratios. However, this simple model seems to be robust enough to give a good first insight. The most likely reasons for deviation from the canonical period ratio value are firstly that sunspots and pores (just like most lower atmospheric magnetic structures) expand with height, causing magnetic stratification (Verth & Erdélyi 2008; Luna-Cardozo et al. 2012), and secondly, that the Sun's gravity causes density stratification (Andries et al. 2009). These two effects will either increase or decrease the period ratio of the harmonics depending on the chosen density or magnetic profile (see Luna-Cardozo et al. 2012,

for a detailed analysis in the context of slow sausage oscillations). In addition, these magnetic structures are rarely purely cylindrical, they can be elliptical (or arbitrary) in shape (see Ruderman & Erdélyi 2009; Morton & Erdélyi 2009) and in most cases are non-axially symmetric. Also, in some cases the flux tube is more suitably described as open-ended at the transition region, which would remove the even harmonics.

5. Conclusions

In this paper we have investigated several magnetic waveguides, with the objective of detecting MHD sausage waves and determining whether they are slow or fast, propagating or standing. Based on the results presented here, we have confidently interpreted the observed periodic changes in the area cross section of flux tubes, which are manifested as a pore and two sunspot waveguide structures, as proof of the existence of linear slow and fast sausage MHD oscillations. Using wavelet analysis, we found standing waves in the photosphere with periods ranging from 4 to 32 minutes. Employing complementary EMD analysis has allowed the MHD modes detected to be identified as a combination of *fast sausage* and *slow sausage* modes, due to the phase behaviour of the area and intensity. It is very likely that these oscillations are *standing harmonics* supported in a flux tube. The period ratio ($P_1/P_{i=2,3}$) of these oscillations indicates strongly that they are part of a group of standing harmonics in a flux tube that is non-homogeneous and is bound by the photosphere and the transition region. Furthermore, there is possible indirect evidence of mode conversion occurring in one of these magnetic waveguides.

Acknowledgements. The authors thank J. Terradas for providing the EMD routine used in the data analysis. RE acknowledges M. Kéray for patient encouragement and is also grateful to NSF, Hungary (OTKA, Ref. No. K83133). This work is supported by the UK Science and Technology Facilities Council (STFC). Wavelet power spectra were calculated using a modified computing algorithms of wavelet transform original of which was developed and provided by C. Torrence and G. Compo, and is available at URL: <http://paos.colorado.edu/research/wavelets/> The DOT is operated by Utrecht University (The Netherlands) at Observatorio del Roque de los Muchachos of the Instituto de Astrofísica de Canarias (Spain) funded by the Netherlands Organisation for Scientific Research NWO, The Netherlands Graduate School for Astronomy NOVA, and SOZOU. The DOT efforts are part of the European Solar Magnetism Network. The SVST was operated by the Institute for Solar Physics, Stockholm, at the Observatorio del Roque de los Muchachos of the Instituto de Astrofísica de Canarias (La Palma, Spain)

References

Andries, J., van Doorselaere, T., Roberts, B., et al. 2009, *Space Sci. Rev.*, 149, 3
 Arregui, I., Oliver, R., & Ballester, J. L. 2012, *Living Reviews in Solar Physics*, 9, 2
 Asai, A., Ishii, T. T., Isobe, H., et al. 2012, *ApJ*, 745, L18
 Banerjee, D., Erdélyi, R., Oliver, R., & OShea, E. 2007, *Sol. Phys.*, 246, 3
 Bogdan, T. J. 2000, *Sol. Phys.*, 192, 373
 Bogdan, T. J. & Judge, P. 2006, *Phil. Trans. R. Soc. London, Ser. A*, 364, 313
 Bonet, J., Márquez, I., Muller, R., Sobotka, M., & Roudier, T. 2005, *A&A*, 430, 1089
 Christopoulou, E. B., Georgakilas, A. A., & Koutchmy, S. 2000, *A&A*, 354, 305
 Cooper, F. C., Nakariakov, V. M., & Tsiklauri, D. 2003a, *A&A*, 397, 765
 Cooper, F. C., Nakariakov, V. M., & Williams, D. R. 2003b, *A&A*, 409, 325
 de Moortel, I. 2009, *Space Sci. Rev.*, 149, 65
 Dorotovič, I., Erdélyi, R., & Karlovský, V. 2008, in *Proc. IAU Symposium No. 247*, ed. R. Erdélyi & C. A. Mendoza-Briceño, Vol. 247 (Cambridge University Press), 351
 Edwin, P. M. & Roberts, B. 1983, *Sol. Phys.*, 88, 179
 Erdélyi, R. 2008, in *Physics Of The Sun And Its Atmosphere*, ed. B. N. Dwivedi & U. Narain
 Fedun, V., Shelyag, S., & Erdélyi, R. 2011a, *ApJ*, 727, 17

Fedun, V., Shelyag, S., Verth, G., Mathioudakis, M., & Erdélyi, R. 2011b, *Ann. Geophys.*, 29, 1029
 Fujimura, D. & Tsuneta, S. 2009, *ApJ*, 702, 1443
 Gary, G. 2001, *Sol. Phys.*, 203, 71
 Goedbloed, J. P. & Poedts, S. 2004, *Principles of magnetohydrodynamics: With applications to laboratory and astrophysical plasmas* (Cambridge Univ Press)
 Huang, N., Shen, Z., Long, S., et al. 1998, *Proc. R. Soc. A*, 454, 903
 Jess, D., Mathioudakis, M., Erdélyi, R., et al. 2009, *Science*, 323, 1582
 Khomenko, E., Collados, M., & Felipe, T. 2008, *Sol. Phys.*, 251, 589
 Kobanov, N. I., Kolobov, D., & Makarchik, D. V. 2006, *Sol. Phys.*, 238, 231
 Luna-Cardozo, C., Verth, G., & Erdélyi, R. 2012, *ApJ*, 748, 110
 Malins, C. & Erdélyi, R. 2007, *Sol. Phys.*, 246, 41
 Mathew, S. K. 2008, *Sol. Phys.*, 251, 515
 McAteer, R., Gallagher, P., Williams, D., et al. 2003, *ApJ*, 587, 806
 Morton, R. & Erdélyi, R. 2009, *A&A*, 502, 315
 Morton, R. J., Erdélyi, R., Jess, D. B., & Mathioudakis, M. 2011, *ApJ*, 729, L18
 Pintér, B. & Erdélyi, R. 2011, *Space Sci. Rev.*, 1
 Ruderman, M. S. & Erdélyi, R. 2009, *Space Sci. Rev.*, 149, 199
 Rutten, R., Hammerschlag, R., Bettonvil, F., Sütterlin, P., & De Wijn, A. 2004, *A&A*, 413, 1183
 Scharmer, G., Brown, D., Pettersson, L., & Rehn, J. 1985, *Applied Optics*, 24, 2558
 Terradas, J., Oliver, R., & Ballester, J. 2004, *ApJ*, 614, 435
 Thompson, M. J. 2006, *Phil. Trans. R. Soc. London, Ser. A*, 364, 297
 Torrence, C. & Compo, G. 1998, *Bulletin of the American Meteorological Society*, 79, 61
 Verth, G. & Erdélyi, R. 2008, *A&A*, 486, 1015
 Wang, T. 2011, *Space Sci. Rev.*, 158, 397